

## High Field Magnetization in Manganese Intermetallic Compounds(Magnetism)

著者	Kanomata Takeshi, Abe Shunya, Kaneko Takejiro, Nakagawa Yasuaki
journal or publication title	Science reports of the Research Institutes, Tohoku University. Ser. A, Physics, chemistry and metallurgy
volume	38
number	2
page range	196-205
year	1993-06-30
URL	<a href="http://hdl.handle.net/10097/28436">http://hdl.handle.net/10097/28436</a>

High Field Magnetization in Manganese Intermetallic Compounds<sup>\*</sup>

Takeshi Kanomata<sup>a</sup>, Shūnya Abe<sup>b</sup>, Takejiro Kaneko<sup>b</sup> and Yasuaki Nakagawa<sup>b</sup>

<sup>a</sup> Faculty of Engineering, Tohoku Gakuin University, Tagajo

<sup>b</sup> Institute for Materials Research, Tohoku University, Sendai

(Received January 18, 1993 )

Synopsis

Magnetization measurements were carried out on manganese intermetallic compounds  $Mn_3MC$  ( $M=Ga, Zn$ ),  $Mn_{2-x}Co_xSb$  ( $x=0.09$  and  $0.15$ ) and  $MnMX$  ( $M=Ru, Rh, Pd; X=As, P$ ) in magnetic fields up to 150 or 320 kOe. Antiferromagnetic (AF)-ferromagnetic (F) field-induced transitions and (AF+F)-(F) one were observed for  $Mn_3GaC$  and  $Mn_3ZnC$ , respectively. For  $Mn_{1.91}Co_{0.09}Sb$ , intermediate (I)-ferrimagnetic (Fr) field-induced transitions were observed. For  $Mn_{1.85}Co_{0.15}Sb$ , AF-Fr field-induced transitions were observed. These transitions were of the first order except one of  $Mn_3ZnC$ . The magnetic properties of  $MnMX$  ( $M=Ru, Rh, Pd; X=As, P$ ) were discussed on the basis of the values of magnetization and high-field magnetic susceptibility.

I. Introduction

Ternary manganese compounds  $Mn_3MX$  ( $M=Ga, Zn, Al, Sn$  and  $In; X=C$  and  $N$ ) have the cubic perovskite structure. Their magnetic properties have been extensively studied because they show magnetic moments, magnetic structures and magnetic transitions characteristic of itinerant electron magnets in great variety.<sup>1,2)</sup> The magnetic properties of  $Mn_3GaC$  are characterized by an AF-F first-order transition at the transition temperature ( $T_t$ ) which is approximately 170 K at zero field. The AF state below  $T_t$  has the magnetic structure of a  $(\pi \pi \pi)$ -type. The magnetic moment of Mn is  $\mu_{Mn}=1.8 \mu_B$  at 4.2 K. The Curie temperature ( $T_c$ ) of the F state is about 255 K.  $Mn_3ZnC$  also shows the transition between magnetically ordered states at  $T_t \sim 230K$ . Neutron diffraction studies show that both AF and F state coexist below  $T_t$ . The magnetic structure is tetragonal noncollinear with a F component along the tetragonal [001] axis and an AF component in the (001) plane. It is noticed that the magnetic moment on the AF sublattice is  $2.7 \mu_B$  and much larger than  $1.6 \mu_B$  on the F sublattice at 4.2 K. The transition from an (AF+F) to F state at  $T_t$  is of the second order.

---

<sup>\*</sup> The 1921th report of Institute for Materials Research

The intermetallic compounds  $Mn_{2-x}Co_xSb$  ( $x < 0.37$ ) crystallize in the tetragonal  $Cu_2Sb$ -type structure.  $Mn_2Sb$  is a ferrimagnet with a Neel temperature of 550 K. The spin ordering of the Fr state for  $Mn_2Sb$  is an antiparallel arrangement of unequal magnetic moments associated with two kinds of manganese atoms ( $Mn_I$  and  $Mn_{II}$ ), where the  $Mn_I$  and  $Mn_{II}$  atoms have magnetic moments of  $2.1 \mu_B$  and  $3.9 \mu_B$  at 0 K, respectively. The magnetic moments are perpendicular to the  $c$  axis below 240 K and parallel to that axis above 240 K. Bither et al,<sup>3)</sup> and Kanomata and Ido<sup>4)</sup> observed that substitution of Co in  $Mn_2Sb$  results in a magnetic transition from a Fr to an AF state with decreasing temperature. According to the results of the magnetic measurements for  $Mn_{2-x}Co_xSb$ , the compounds with  $0.10 < x < 0.35$  exhibits a first-order AR-Fr phase transition at  $T_t$  which accompanies the discontinuous change of lattice constants  $a$  and  $c$ . For the compounds with  $0.06 < x < 0.10$ , an I phase appears at low temperatures and the first order phase transitions from the I state to the Fr one have been observed with increasing temperature.

The ternary intermetallic compounds  $MnMX$  ( $M=Ru, Rh, Pd; X=As, P$ ) crystallize into the hexagonal  $Fe_2P$ -type structure. In the  $Fe_2P$ -type structure, the non-metal atoms form tetrahedra and square-based pyramids both stacked in triangular channels along the hexagonal  $c$  axis. The 4d atoms are located on the tetrahedral sites of one channels and Mn atoms on the pyramidal sites of adjacent channels. The compounds  $MnRhAs$  and  $MnRuP$  have been extensively investigated because of their interesting magnetic properties<sup>5,6)</sup> which have magnetic order-order transition from the AF state to the AF+F coexistent one of the antiferromagnetic and ferromagnetic components of magnetic moment (canted state) for  $MnRhAs$  and from the AF1 state to the AF2 one for  $MnRuP$ . The compounds  $MnRuAs$  and  $MnRhP$  are ferromagnets. Recently, the magnetic and electrical properties of the compounds  $MnMX$  ( $M=Ru, Rh, Pd; X=As, P$ ) have been studied by Kanomata et al<sup>7)</sup> and Harada et al.<sup>8)</sup> Their magnetic properties are summarized in Table 1.

Table 1 Magnetic data of ternary compounds  $MnMX$  ( $M=Ru, Rh, Pd; X=As, P$ ) from refs. (6) and (7).

Compound	Magnetic order	$T_C, T_N, T_f$ or $T_t$ (K)
MnRuAs	F	496K ( $T_C$ )
MnRhAs	AF1/Cant/AF2?	160 ( $T_t$ ), 200 ( $T_C$ )
MnPdAs	Cant?	210 ( $T_C$ )
MnRuP	AF1/AF2/AF3	116 ( $T_t$ ), 176 ( $T_t$ ), 296 ( $T_N$ )
MnRhP	F	401 ( $T_C$ )
MnPdP	Spin-glass?	26 ( $T_f$ )

As stated above, the magnetic moments of the Mn atoms in  $Mn_3MC$  ( $M=Ga, Zn$ ) and  $Mn_{2-x}Co_xSb$  are much smaller than about  $4 \mu_B$  observed in other ordered manganese alloys, in which the magnetic moment of Mn is considered to be localized, and their magnitude depend strongly on the magnetic states. Therefore, the magnetic properties of these compounds are considered to be interpreted in terms of an itinerant-electron magnetism. This is also supported by the band calculations<sup>9-12)</sup> for these compounds. The band structures calculated for MnCoP show that the 3d bandwidth is fairly wide.<sup>13)</sup> This means that the d electrons for MnCoP should be treated as itinerant electrons. So, it is considered that the magnetic properties of the compounds  $MnMX$  ( $M=Ru, Rh, Pd; X=As, P$ ) should be also interpreted in terms of the itinerant-electron magnetism. We have studied the magnetic properties of  $Mn_3MC$  ( $M=Ga, Zn$ ),<sup>2, 14)</sup>  $Mn_{2-x}Co_xSb$ <sup>15)</sup> and  $MnMX$  ( $M=Ru, Rh, Pd; X=As, P$ )<sup>16, 17)</sup> under high field. Our results are reviewed here from the viewpoint of itinerant electron magnetism.

## II. Experimental Results and Discussions

### 1. $Mn_3MC$ ( $M=Ga, Zn$ )

Figure 1 shows the temperature dependence of specific magnetization ( $\sigma_g$ ) and reciprocal magnetic susceptibility per mole ( $1/\chi_{mol}$ ) for  $Mn_3MC$  ( $M=Ga, Zn$ ). As seen in the figure, the magnetic order-order transitions occur at 165 K and 215 K for  $Mn_3GaC$  and  $Mn_3ZnC$ , respectively. The field-induced transitions were examined at various temperatures below these transition temperatures.<sup>14)</sup> As an example the magnetization curve at  $Mn_3GaC$  at 4.2 K is shown in Fig.2, in which a field-induced transition from an AF to F state takes place around 200 kOe with increasing field. There is observed a large hysteresis and ( $H_C - H_C$ ) is 50 kOe. The magnetization in the F state is  $\sigma_g = 70$  emu/g, which gives  $\mu_{Mn} = 1.0 \mu_B$ . It should be noted that the value of  $\mu_{Mn}$  in the F state is much smaller than  $1.8 \mu_B$  in the AF state. This reduction of magnetic moment is ascribed to the volume contraction caused by the field-induced AF - F transition. All the field-induced transitions from the AF to F state below  $T_t$  were found to be of the first order. The temperature variations of the transition fields are shown in Fig.3(b). The value of  $dH_C/dT$  just below  $T_t$  is estimated to be  $-2.3$  kOe/K. The entropy change at  $T_t$ ,  $\Delta S$ , can be deduced from the Clausius-Clapeyron equation,  $\Delta S = -(dH_C/dT) \Delta \sigma$ .  $\Delta S$  is estimated to be  $0.42R$  ( $R$  is the gas constant) which is consistent with  $0.5R$  obtained from the specific heat measurement.<sup>18)</sup> For  $Mn_3ZnC$ , no abrupt change of magnetization was observed at the field-induced transition from an (AF+F) to F state and the field-induced transition is of the second order. The  $H_C$  versus  $T$  curve is shown in Fig.3(d).

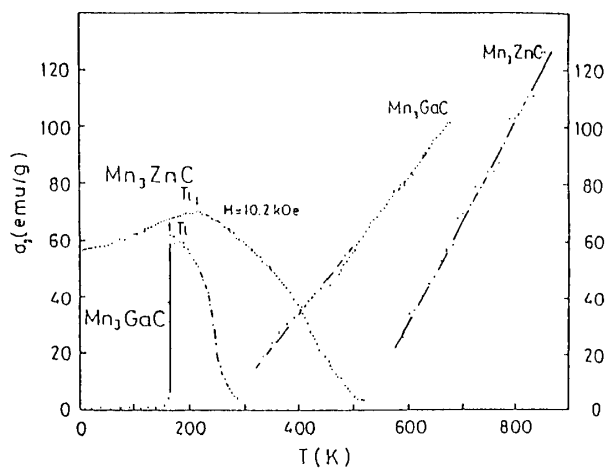


Fig. 1 Thermomagnetic curves for  $Mn_3MC$  ( $M=Ga$  and  $Zn$ )<sup>2)</sup>

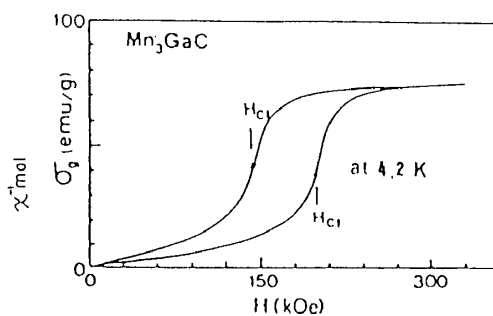


Fig. 2 Magnetization curves for  $Mn_3GaC$ <sup>14)</sup>

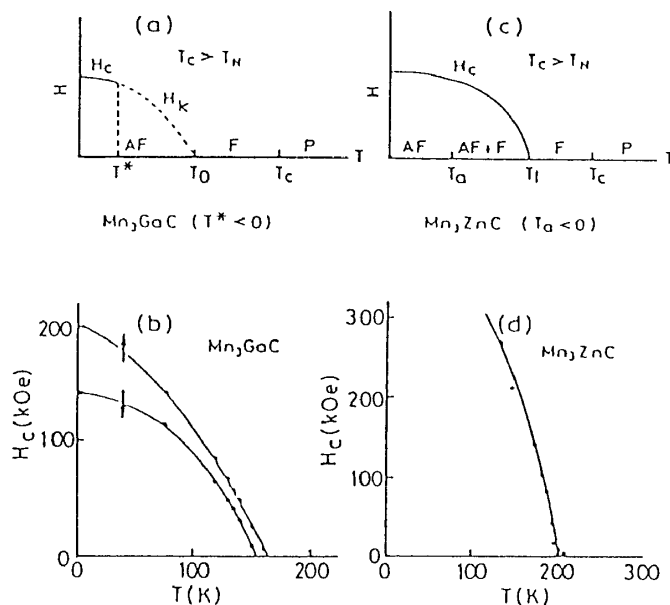


Fig. 3 Temperature dependence of critical field for  $Mn_3GaC$  and  $Mn_3ZnC$ .<sup>2)</sup>

As stated in the section I, in the present compounds the amplitude of local spin density at Mn atoms is variable. There occur the coexistence of ferromagnetism and antiferromagnetism, and also a transition between them. Moriya and Usami showed that a coexistence of ferro- and antiferromagnetism and a phase transition between magnetically ordered states takes place in itinerant electron system on the basis of SCR theory of spin fluctuation.<sup>19)</sup> According to the theory, in the itinerant electron system without magnetic anisotropy the free energy  $F$  as a function of uniform ( $M_0$ ) and staggered ( $M_Q$ ) components of magnetization is expressed as follows,

$$F = (1/2 \chi_0) M_0^2 + (1/2 \chi_Q) M_Q^2 + (1/4) \gamma_u M_0^4 + (1/4) \gamma_s M_Q^4 + (1/2) \gamma_{us} M_0^2 M_Q^2 - HM$$

where  $H$  is the uniform external field,  $\chi_0$  and  $\chi_Q$  are the uniform and staggered susceptibility, respectively, and  $\gamma$ 's are coefficients of 4th power of magnetization. The temperature dependence of  $1/\chi_0$  and  $1/\chi_Q$  are dominated by the effect of correlated spin fluctuations. In the F(AF) system  $1/\chi_0$  and  $1/\chi_Q$  pass through zero as  $T$  is changed.  $T_c$  and  $T_N$  are defined as  $1/\chi_0(T_c) = 0$  and  $1/\chi_Q(T_N) = 0$ . When the temperature dependence of  $\gamma$ 's is neglected, four different phase diagrams are derived by minimizing the free energy. Two of them are shown in Fig.3(a) and (c). The diagram(a) appears when the mode-mode coupling is strong ( $\gamma_{us} > \gamma_u \gamma_s$ ) and (c) when the coupling is weak ( $\gamma_{us} < \gamma_u \gamma_s$ ).  $T_0$ ,  $T_a$  and  $T_f$  are defined by  $\chi_Q/\chi_0(T_0) = (\gamma_u/\gamma_s)^{1/2}$ ,  $\chi_Q/\chi_0(T_a) = \gamma_{us}/\gamma_s$  and  $\chi_Q/\chi_0(T_f) = \gamma_u/\gamma_{us}$ , respectively.  $H_c$  and  $H_k$  are the critical fields, at which the second order and the first order phase transitions take place, respectively. It is thought that the phase diagram (b) for  $Mn_3GaC$  corresponds to the diagram (a) with  $T < 0$  and the phase diagram(d) for  $Mn_3ZnC$  to the diagram(c) with  $T_a < 0$ . The magnetic moment in the field-induced F state in  $Mn_3GaC$  is much smaller than that in the AF state at 4.2 K. This can be understood in terms of itinerant electron magnetism, because the large volume contraction caused by the field-induced AF-F transition broadens the electronic band and consequently reduces the moment. A study of magnetostriction under high field for  $Mn_3GaC$  is in progress.

## 2. $Mn_{2-x}Co_xSb$

Figure 4 and 5 show the magnetization  $\sigma$  versus field at various temperatures for  $Mn_{1.91}Co_{0.09}Sb$  and  $Mn_{1.85}Co_{0.15}Sb$ , respectively.<sup>15)</sup> The field-induced metamagnetic phase transitions from the I to the Fr state and from the AF to the Fr state were observed for  $Mn_{1.91}Co_{0.09}Sb$  and  $Mn_{1.85}Co_{0.15}Sb$ , respectively. The field-induced transition fields,  $H_{c\uparrow}$  and  $H_{c\downarrow}$ , are defined as shown with arrows in the figure. The first order magnetic transition of  $Mn_{1.85}Co_{0.15}Sb$  takes place between the spin structures of the  $Mn_2As$ - and  $Mn_2Sb$ -types. Figures 6 and 7 show the temperature dependence of magnetization for  $Mn_{1.91}Co_{0.09}Sb$  and  $Mn_{1.85}Co_{0.15}Sb$ , respectively. For  $Mn_{1.85}Co_{0.15}Sb$ , the magnetization in the temperature range from 120 to 200 K in a field of 150 kOe is  $\sim 20\%$  higher than the saturation magnetization of  $Mn_2Sb$  in the same temperature range. In the temperature range from 5.9 to 135 K in a field of 150 kOe, the magnetizations of  $Mn_{1.91}Co_{0.09}Sb$  are  $\sim 30\%$  higher than the saturation magnetization of  $Mn_2Sb$  in the same temperature range. By extrapolating the magnetization versus temperature curves at 150 kOe in the Fr state to 0 K in Figs.6 and 7, averaged magnetic moments are defined to be  $2.2 \mu_B$  and  $\sim 2.2 \mu_B$  for  $Mn_{1.91}Co_{0.09}Sb$  and  $Mn_{1.85}Co_{0.15}Sb$ , respectively. The

increase of moment by substitution of Mn for Co is explained by assuming that nonmagnetic Co atoms occupy site I and the magnetic moments of  $Mn_I$  and  $Mn_{II}$  atoms have value equal to those of  $Mn_2Sb$  in the pseudobinary system  $Mn_{2-x}Co_xSb$ . The temperature variations of the observed transition fields are

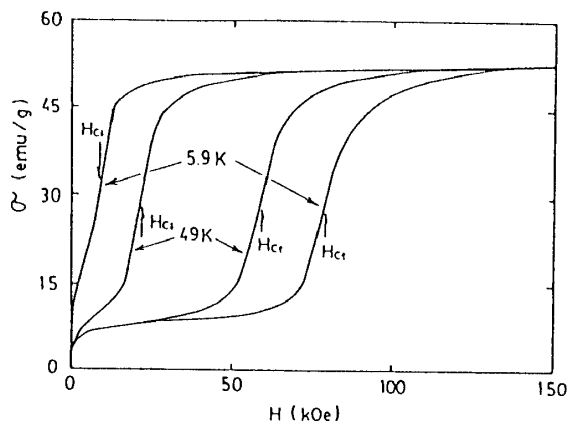


Fig.4 Magnetization curves at various temperatures for  $Mn_{1.91}Co_{0.09}Sb$ .

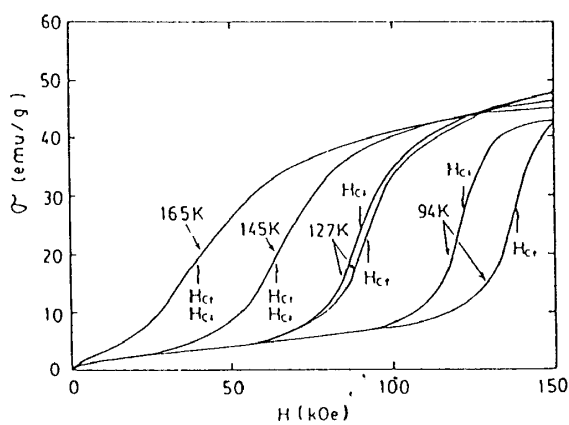


Fig.5 Magnetization curves at various temperatures for  $Mn_{1.85}Co_{0.15}Sb$ .

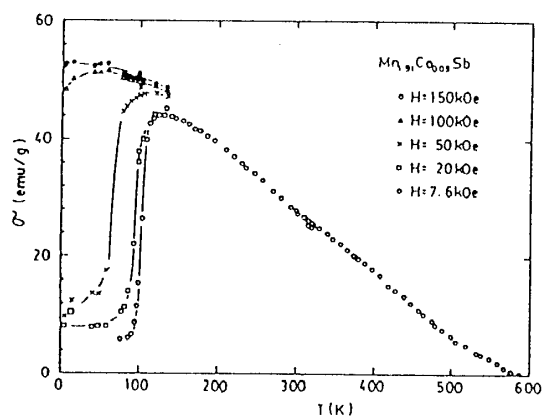


Fig.6 Thermomagnetic curves in various fields for  $Mn_{1.91}Co_{0.09}Sb$ .

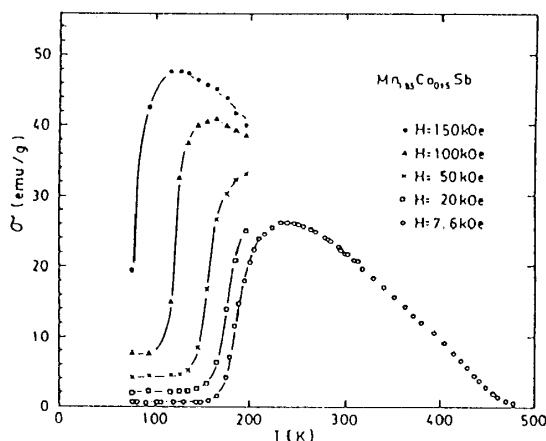


Fig.7 Thermomagnetic curves in various fields for  $Mn_{1.85}Co_{0.15}Sb$ .

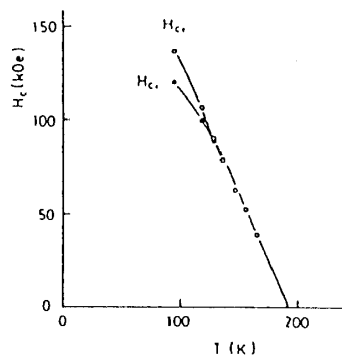


Fig.8 Transition field versus temperature for  $Mn_{1.85}Co_{0.15}Sb$ .

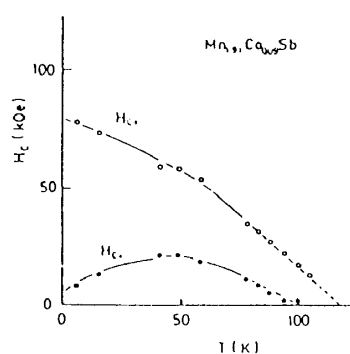


Fig.9 Transition field versus temperature for  $Mn_{1.91}Co_{0.09}Sb$ .

shown in Figs. 8 and 9 for  $\text{Mn}_{1.85}\text{Co}_{0.15}\text{Sb}$  and  $\text{Mn}_{1.91}\text{Co}_{0.09}\text{Sb}$ , respectively. The values of  $dH_c/dT$  just below  $T_t$  are estimated to be  $-0.86$  kOe/K and  $-1.42$  kOe/K for  $\text{Mn}_{1.91}\text{Co}_{0.09}\text{Sb}$  and  $\text{Mn}_{1.85}\text{Co}_{0.15}\text{Sb}$  from the temperature variations of the observed transition fields, respectively. Using Clausius-Clapeyron's equation, the total entropy change  $\Delta S$  at  $T_t$  of  $\text{Mn}_{1.91}\text{Co}_{0.09}\text{Sb}$  and  $\text{Mn}_{1.85}\text{Co}_{0.15}\text{Sb}$  are estimated to be  $0.11R$  and  $0.17R$ , using the values of  $dH_c/dT$  and  $\Delta\sigma$ , respectively. The main sources of these large entropy change at  $T_t$  was considered to be ascribed to the magnetic contribution at the  $\text{Mn}_{\text{II}}$  site. In fact, the AF-Fr phase transition is accompanied by a change in the magnetic moment of the Mn atoms according to the results of neutron diffraction for  $\text{Mn}_{1.80}\text{Co}_{0.20}\text{Sb}$ .<sup>20)</sup> In particular, the magnetic moment on the  $\text{Mn}_{\text{II}}$  atoms is found to be  $\sim 3.4 \mu_B$  just below  $T_t$  and  $\sim 2.4 \mu_B$  just above  $T_t$ .

Recently, Chonan et al.<sup>11)</sup> and Suzuki et al.<sup>12)</sup> calculated the band structure of  $\text{Mn}_2\text{Sb}$  by a self-consistent augmented plane wave method. According to their calculation, the density of states consists of three parts: bonding and antibonding d-p bands and a nonbonding d-band with the Fermi level lying in the nonbonding band. The non-bonding d band width is about 3-4 eV, which is fairly wide. Therefore, these authors concluded that the d electrons of Mn atoms should be treated not as localized electrons, but as itinerant electrons. Thus, it is considered that the magnetic properties of  $\text{Mn}_{2-x}\text{Co}_x\text{Sb}$  should be discussed in terms of the itinerant-electron magnetism. General theories of magnetic transitions in an itinerant-electron system were proposed by Moriya and Usami<sup>19)</sup> and Isoda<sup>21)</sup> on the basis of spin fluctuation. However, the transitions from the I to the Fr state and the AF to the Fr state observed for  $\text{Mn}_{2-x}\text{Co}_x\text{Sb}$  do not occur in both the theories mentioned above. A further experimental and theoretical investigation of the magnetic order-order transition will be necessary.

### 3. $\text{MnMX}$ ( $M=\text{Ru, Rh, Pd}$ ; $X=\text{As, P}$ )

Figure 10 shows the magnetization curves of  $\text{MnRuAs}$  ( $T=5.5$  K) and  $\text{MnPdAs}$  ( $T=8$  K) together with that of  $\text{MnRhAs}$  ( $T=4.2$  K). Figure 11 shows the magnetization curve of  $\text{MnRhP}$ . The magnetization of the ferromagnet  $\text{MnRuAs}$  was saturated at magnetic fields above 50 kOe and the spontaneous magnetization ( $\sigma_s$ ) was found to be  $21.5 \times 10^3$  emu/mol giving the magnetic moment per Mn atom of  $\mu_{\text{Mn}}=3.9 \mu_B$  provided the moments are located at Mn atoms only. The high field susceptibility was found to be  $\chi_{\text{hf}}=1.7 \times 10^{-3}$  emu/mol. The magnetization of the ferromagnet  $\text{MnRhP}$  was saturated above 25 kOe and the spontaneous magnetization was found to be  $17 \times 10^3$  emu/mol giving  $\mu_{\text{Mn}}=3 \mu_B$ . Thus, the value of the magnetic moment per Mn atom in  $\text{MnRhP}$ ,  $3 \mu_B$ , is smaller by about  $1 \mu_B$  compared with  $3.9 \mu_B$  in  $\text{MnRuAs}$ . The previous results show that the



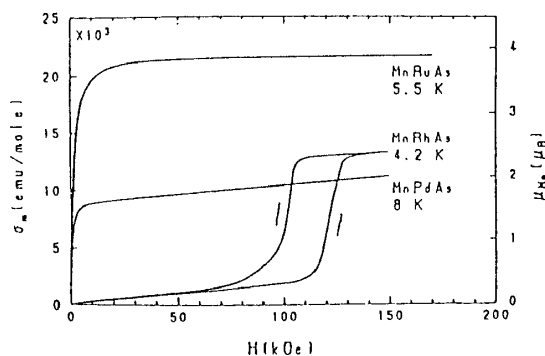


Fig.10 Magnetization curves of MnRuAs, MnRhAs and MnPdAs.<sup>16)</sup>

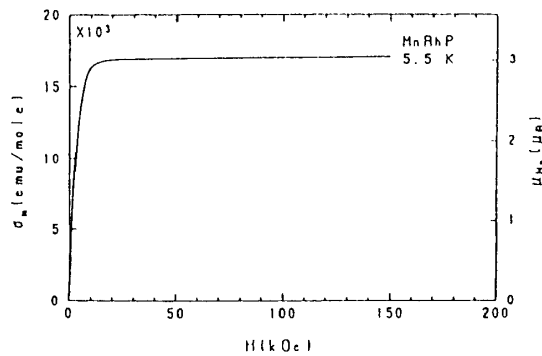


Fig.11 Magnetization curve of MnRhP.<sup>16)</sup>

magnetic moment of the Mn atom at the pyramidal site in manganese compounds with the crystal structure of  $\text{Fe}_2\text{P}$ -,  $\text{Co}_2\text{P}$ - and  $\text{Cu}_2\text{Sb}$ -type is usually about  $3 \mu_B$  in the phosphide and about  $4 \mu_B$  in the arsenides. The values of  $\mu_{\text{Mn}}$  in MnRuAs and MnRhP obtained in this experiment agree well with those expected for the arsenides and phosphides, respectively. The magnetization of MnRhAs shows an abrupt increase around 80 kOe.<sup>17)</sup> This discontinuous increase of  $\sigma$  corresponds to the field-induced transition from the AF state to the canted (AF+F) state. The extrapolation of the magnetization curve after the transition to  $H=0$  intersects the  $\sigma$  axis at  $11 \times 10^3 \text{ emu/mol}$ , which gives  $\mu_{\text{Mn}} = 2.0 \mu_B$ .  $\chi_{\text{hf}}$  was estimated to be  $15 \times 10^{-3} \text{ emu/mol}$ . The magnetization of MnPdAs appears to be saturated above about 15 kOe with large high field susceptibility. The spontaneous magnetization was found to be  $9 \times 10^3 \text{ emu/mol}$  giving  $\mu_{\text{Mn}} = 1.6 \mu_B$ .  $\chi_{\text{hf}}$  was estimated to be  $15 \times 10^{-3} \text{ emu/mol}$ . Thus, the values of  $\mu_{\text{Mn}}$  obtained for MnRhAs and MnPdAs are almost the same, but much smaller than those for the ferromagnets MnRuAs and MnRhP. Furthermore, the values of  $\chi_{\text{hf}}$  for MnRhAs and MnPdAs are the same, but much larger than those for MnRuAs and MnRhP. The values of  $\mu_{\text{Mn}}$  and  $\chi_{\text{hf}}$  for MnRhAs were obtained from the magnetization of the field-induced canted state. The similar values of  $\mu_{\text{Mn}}$  and  $\chi_{\text{hf}}$  obtained for MnRhAs and MnPdAs suggest that MnPdAs is also in the canted state. The large values of  $\chi_{\text{hf}}$  for MnRhAs and MnPdAs can be ascribed to the existence of canted magnetic moments. Figure 12 shows the magnetization curves for the antiferromagnet MnRuP. The magnetization curves below 77 K did not show any field dependence of magnetic susceptibility. The magnetization curve at 150 K just below  $T_t$  showed the existence of a field-induced transition at fields between 70 and 100 kOe, where the magnetization curves have hysteresis. At 227 K, between  $T_t$  and  $T_N$ , the magnetization increases almost linearly with the field. Figure 13 shows the magnetization curves for MnPdP. In the magnetization process for MnPdP, the remanent magnetization was observed at 8 K but not at 41.5 K. According to Kanomata et al.<sup>17)</sup>, MnPdP shows spin-glass-like freezing with the freezing

temperature ( $T_t$ ) of 26 K. The remanent magnetization was observed in the magnetization curve at low temperature and found to disappear around  $T_t$ . This result is consistent with an occurrence of spin-glass freezing below  $T_t$  in ref.7.

The transition from the AF state to the AF+F one observed for MnRhAs does not occur in the theories<sup>19,21)</sup> on the basis of the itinerant-electron magnetism. A further investigation of magnetic transitions will be also necessary experimentally and theoretically for MnMX (M=Ru,Rh,Pd;X=As,P) systems.

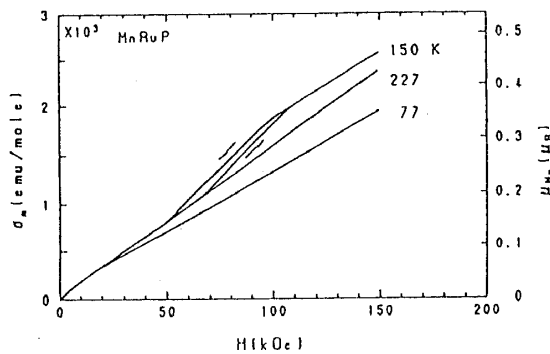


Fig.12 Magnetization curves of MnRuP.<sup>16)</sup>

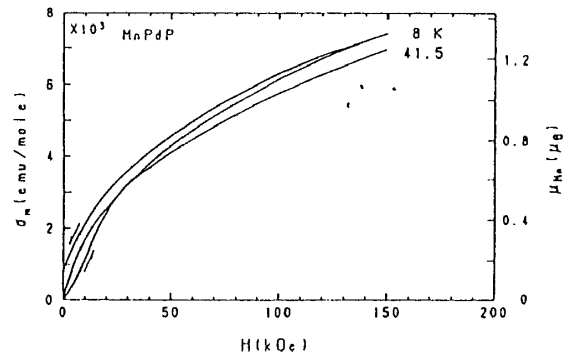


Fig.13 Magnetization curves of MnPdP.<sup>16)</sup>

#### Acknowledgement

The authors would like to thank Professor K.Motizuki, Shinshu University, and Professor N.Suzuki and Dr M.Shirai, Osaka University, for valuable discussions about our studies. A part of this work was carried out under the Interuniversity Cooperative Research Program of the Institute for Materials Research, Tohoku University and measurements were done at High Field Laboratory for Superconducting Materials, Institute for Materials Research, Tohoku University.

#### References

- 1) D.Fruchart and E.F.Bertaut, J.Phys.Soc.Jpn.44(1978)781 and references cited therein.
- 2) T.Kaneko, T.Kanomata and K.Shirakawa, J.Phys.Soc.Jpn. 56(1987) 4047 and references cited therein.
- 3) T.A.Bither, P.H.Walter, W.H.Cloud, T.J.Swoboda and P.E.Bierstedt J.Appl.Phys.33(1962)1346.

- 4) T.Kanomata and H.Ido, *J.Appl.Phys.* 55(1984)2039.
- 5) B.Chenevier, J.Baruchel, M.Bacmann, D.Fruchart and R.Fruchart, *J.Allys.Comp.*, 179(1992)147 and references cited therein.
- 6) J.Bartolome, J.Garcia, C.Rillo, E.Paracios, M.Bacmann, D.Fruchart, R.Fruchart and B.Chenevier, *J.Magn.Magn.Mater.* 54-57(1986) 1499.
- 7) T.Kanomata, T.Kawashima, H.Utsugi, T.Goto, H.Hasegawa and T.Kaneko, *J.Appl.Phys.* 69(1991) 4639.
- 8) T.Harada, T.Kanomata and T.Kaneko, *J.Magn.Magn.Mater.* 90&91(1990) 169.
- 9) K.Motizuki and H.Nagai, *J.Phys.C21* (1988)5251.
- 10) K.Motizuki, H.Nagai and T.Tanimoto, *J.Phys.Colloq. (Franc)* 49(1988)C8-161.
- 11) T.Chonan, M.Shirai and K.Motizuki, *J.Phys.Soc.Jpn.* 60(1991)1638.
- 12) M.Suziki, M.Shirai and K.Motizuki, *J.Phys.Condens.Matter* 4(1992)L33.
- 13) S.Fujii, S.Ishida and S.Asano, *J.Phys.F.* 18(1988) 971.
- 14) T.Kaneko, T.Kanomata, S.Miura, G.Kido and Y.Nakagawa, *J.Magn.Magn.Mater.* 70(1987)261.
- 15) T.Kanomata, Y.Hasebe, T.Kaneko, S.Abe and Y.Nakagawa, *Physica B* 177(1992)119.
- 16) T.Kaneko, T.Kanomata, T.Kawashima, S.Mori, S.Miura and Y.Nakagawa, *Physica B* 177(1992)123.
- 17) T.Kaneko, H.Yasui, Y.Nakagawa and T.Kanomata, *J.Magn.Magn.Mater.* 104-107(1992)1949.
- 18) J.Garcia, J.Bartolome, D.Gonzalez, R.Navarro and D.Fruchart, *J.Chem.Thermodynamics* 15(1983)1059.
- 19) T.Moriya and K.Usami, *Solid State Commun.* 23(1977)935.
- 20) M.Ohashi, Y.Yamaguchi and T.Kanomata, *J.Magn.Magn.Mater.* 104 (1992)925.
- 21) M.Isoda, *J.Phys.Soc.Jpn.* 53(1984)3587.